diminish higher in the Rydberg series, we averaged together the excitation energies for all the symmetry components arising from an individual 2e → *n*e excitation. The results are shown in Table VI. While the splitting among the 3d members is less than that in the 3p states, in neither case is the designation (σ, π, δ) (e.g., 3pπ) valid, as it would be in the case of a linear molecule. In addition, the $\pi \rightarrow 3p\pi$ "state" is slightly lower than the $\pi \rightarrow 3p\sigma$ "state", due to valence $\pi \rightarrow \pi^*$ mixing in the 1^1B_2 state. In the d series, we have $\sigma < \pi < \delta$ as in the usual case, although these are not "good" quantum numbers. Similar averaging over the states designated σ, π, δ, etc. lead to the calculated quantum defects, $\delta_s = 1.016$, $\delta_p = 0.0692$, and $\delta_d = 0.313$. These are quite reasonable values, although the value of δ_d is larger than is typically the case. However, one must keep in mind that these defects are calculated from the lowest members of the various Rydberg series, and allene is large enough so the lower Rydberg states may lie significantly below the strictly hydrogenic value. Nonetheless, even under such gross assumptions, in every case, peaks in the absorption spectrum are observed (±200 cm^{-1}) where predicted by the Rydberg formula

$$E_n = I - R/(n - \delta)^2 \qquad (12)$$

for each of the series, s, pσ, pπ, dσ, dπ, and dδ through $n \simeq 6$, or 3200 cm^{-1} below the ionization limit. This then seems to provide some real basis for our assignments.

Conclusion

We have calculated the vertical singlet excited states of allene in the 6.5–8.6-eV range. All optically allowed states in this region arise from valence → Rydberg excitations, with the exception of the valence $\pi \rightarrow \pi^*$ transition, which we assign to the band at 8.58 eV (9.06 eV calcd). Calculated oscillator strengths and excitation energies are consistently in good agreement with experiment. In addition, we have calculated the theoretical MCD parameters A and B for all the excited states in this region. All degenerate ^1E states are found to have small magnetic moments. The magnetic moment of the highest filled 2e orbital is also small, due to delocalization effects. All optically allowed excited states (except the 2^1B_2 state at 8.34 eV) have large B terms. Therefore, all of these states, degenerate or not, would show a nondispersive MCD signal (i.e., would appear nondegenerate). The theoretical MCD spectrum also is in agreement with experiment; the only unexplained feature in either the absorption or MCD spectra (the narrow bands beginning at 172 nm) is probably due to vibronic coupling between the 2^1A_1 and 2^1E states or Jahn–Teller splitting of the 2^1E state itself. The four singlet states arising from the $\pi \rightarrow \pi^*$ excitation are in order $1^1A_2 < 1^1B_1 < 4^1A_1 < 3^1B_2$. All other states in this region are $\pi \rightarrow$ Rydberg excitations. The resulting analysis of the Rydberg series leads to reasonable quantum defects. Higher members of each Rydberg series are found in the absorption spectrum. Outside of the observed MCD at 7.3 eV, it does not appear to be necessary to include the effects of nonvertical geometries in order to interpret either the absorption or MCD spectrum of allene.

Acknowledgment. We gratefully acknowledge the support of the National Science Foundation, Grant CHE-81-06016.

Registry No. Allene, 463-49-0.

S_N2 Reactions in the Gas Phase. Temperature Dependence of the Rate Constants and Energies of the Transition States. Comparison with Solution

Gary Caldwell, Tom F. Magnera, and Paul Kebarle*

Contribution from the Department of Chemistry, University of Alberta, Edmonton, Alberta, Canada T6G 2G2. *Received March 28, 1983*

Abstract: The rate constants for the gas-phase reactions $Cl^- + RBr = ClR + Br^-$, where R = Me, Et, *n*-Bu, *i*-Pr, and *i*-Bu, were determined for temperatures between 25 and 390 °C with a pulsed electron beam high ion source pressure mass spectrometer. The rate constants for Me decreased with an increase of temperature (negative temperature dependence). Et and *n*-Bu had almost no temperature dependence while *i*-Pr and *i*-Bu had positive temperature dependence. An analysis of the data on the basis of theory provides approximate values for ΔE_0, the energy of the transition state

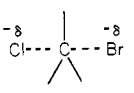

relative to the energy of the reactants. These ΔE_0 values are as follows: Me, −2.5; Et, 0.8; *n*-Bu, −0.5; *i*-Pr, +5.1; *i*-Bu, +5.7 kcal/mol. The $\delta\Delta E_0$ are compared with relative activation energies: δE_a in solution (C. K. Ingold and A. J. Parker) and calculated strain energies $\delta\Delta E_{strain}$ due to steric repulsions in the transition state (C. K. Ingold and D. F. DeTar). An approximate agreement between the three sets of data is found. This finding supports the assumption of Ingold that steric effects in the transition state dominate the relative rates of this reaction series. The temperature dependence of the rate constants in the gas phase is of interest to ion–molecule reaction theory. It provides a graphic demonstration for the effect of the central barrier in the double-well reaction coordinate. When ΔE_0 is negative, negative temperature dependence is observed. When $-\Delta E_0$ is small (Me, *n*-Bu) the reaction proceeds with chemical activation at the very low pressures used in ion cyclotron resonance but with near Boltzmann transition-state distribution at the higher pressures used in high-pressure mass spectrometry. When ΔE_0 is positive, the reaction proceeds with positive temperature dependence and boltzmann transition-state distribution.

Studies of the kinetics and mechanism of bimolecular nucleophilic S_N2 reaction 1 have played a fundamental role in the development of physical organic chemistry.[1-5] Many aspects of the structural and solvent effects in protic and aprotic solvents

0002-7863/84/1506-0959$01.50/0

$$X^- + RY = XR + Y^- \quad (1)$$

are believed to be well understood.[4-8] Nevertheless, it is very desirable to have information on the transition state in the absence of solvent since only such information promises a definitive separation of the intrinsic structural effects from the solvent effects. We can take as an example S_N2 reaction 2 where R represents

$$Cl^- + RBr = ClR + Br^- \quad (2)$$

the different alkyl groups such as Me, Et, *n*-Pr, *n*-Bu, *i*-Pr, *i*-Bu, etc. Studies of these reactions led to a classic series of papers by Ingold and Hughes[1,6] dealing with the effect of steric hindrance due to repulsions between the alkyl groups and the halide atoms in transition-state I. The relative energies of differently substituted

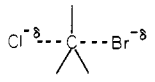

I

species I were estimated by calculating the van der Waals repulsions between the groups, using an empirical repulsive potential. The calculated energies were found in good agreement with the relative activation energies observed in solvents like acetone or *N*,*N*-dimethylformamide.[1,6,7] In the calculations of the relative energies of I no consideration was given to the presence of solvent, i.e., I was treated as an isolated species. Evidently, it is of interest to find out whether the agreement with the solution results is bona fide, i.e., is steric repulsion in I the major factor also in solution, or are solvation energy differences also involved? In the latter case the agreement between the calculations and the solution experiments would be fortuitous.

At the present time the most direct route for obtaining information on the relative energies of the isolated S_N2 transition states would be by quantum mechanical calculations. Unfortunately, series 2 has not been treated so far. However, a number of calculations of S_N2 transition-state energies have been performed.[9] While often the calculations have not been accurate enough to predict good transition-state energies, much useful information has been obtained. A recent example of the value of such calculations is the demonstration of the applicability of the Marcus equation to S_N2 transition states.[10]

Studies of the kinetics of S_N2 reactions 1 and 2 in the gas phase represent another route than can provide information on the transition state in the absence of solvent. However, measurements of the rate constants in the gas phase do not lead directly to the desired information. That is, Arrhenius plots of the temperature dependence of the rate constants do not necessarily lead to the energies of transition-state I. In fact, the interpretation of the experimental rate measurements of gas-phase S_N2 reactions is providing an important contribution to the development of ion–molecule reaction theory. A brief account of the present status, based on recent work,[10-15] is given below.

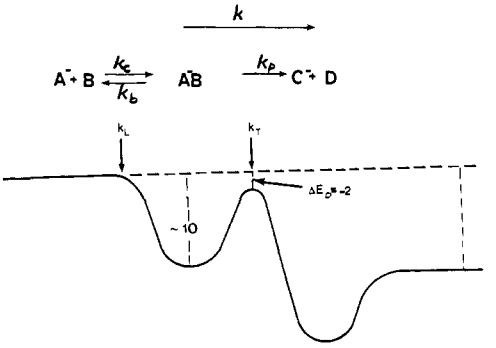

Figure 1. Schematic reaction coordinate for the bimolecular ion–molecule reaction $A^- + B = C^- + D$. There can be two bottlenecks, one at the loose, orbiting collision transition state k_L and the other at the tight, chemical transition state at central barrier k_T. When $-\Delta E_0$ is large (small central barrier), the reaction proceeds at collision rates $k = k_L$ and has essentially no temperature dependence. When $-\Delta E_0$ is small, k_T becomes rate controlling with $k < k_L$, and the reaction has negative temperature dependence. For ΔE_0 positive $k \ll k_L$, and there is positive temperature dependence. The diagram is drawn approximately to scale for energies involved in the reaction $Cl^- + CH_3Br = ClCH_3 + Br^-$. For this case ($A^-B = Cl^-\cdots H_3CBr$), ΔE_0 corresponds to the energy of transition state I.

The reaction coordinate of an exothermic bimolecular ion–molecule reaction is shown in Figure 1. Because of the long range ion–molecule induced dipole and permanent dipole attractive forces, the energy decreases with the approach of A^- and B. At somewhat closer range even stronger attractive forces, like hydrogen bonding, may be present, resulting in the formation of a stable adduct A^-B or Cl^-RBr in the present case. At even shorter distances there will be an increase of energy due to the formation of the chemical transition state, of structure I for the present case. The resulting double potential well with a central barrier is shown in Figure 1.

For such a reaction coordinate there can be two bottlenecks, one at the centrifugal barrier where the loose orbiting transition state is formed and the other at the chemical transition state. The loose Langevin orbiting complex is rate controlling when the top of the central barrier lies low, i.e., when $-\Delta E^\circ$ is large. Under these conditions the reaction is fast, proceeding at orbiting collision rates. There is essentially no temperature dependence and the rate constant equals $k_L \approx k_{ADO} \approx 10^{-9}$ cm^3 molecule^{-1} s^{-1}. No information on the exact energy of the chemical transition state can be obtained for this class of reactions.

When the central barrier is substantial, such that $-\Delta E_0$ is small, the chemical transition state becomes rate controlling. The rate constant is then lower than k_L and is found to decrease with an increase in temperature, i.e., it has negative temperature dependence. The chemical transition state can become rate controlling even though ΔE_0 is negative because the chemical transition state is a tight complex while the orbiting transition state is a loose complex, i.e., the entropy of the chemical transition state is much more unfavorable than that of the orbiting complex.[11]

The chemical transition state is rate controlling, and the rate constants also are much below k_L when ΔE_0 is positive, i.e., when the energy of the central barrier lies higher than that of the reactants. The rate constant in this case shows a positive temperature dependence.[12-15]

(1) Ingold, C. K. "Structure and Mechanism in Organic Chemistry"; 2nd ed.; Cornell University Press: Ithaca, NY; 1969.
(2) Hartshorn, S. R. "Aliphatic Nucleophilic Substitution"; Cambridge University Press: London, 1973.
(3) Alder, R. W.; Baker, R.; Brown, J. M. "Mechanism in Organic Chemistry"; Wiley-Interscience: London, 1971.
(4) Streitwieser, A., Jr. "Solvolytic Displacement Reactions"; McGraw-Hill: New York, 1962.
(5) Amis, E. S.; Hinton, J. F. "Solvent Efects on Chemical Phenomena"; Academic Press: New York, 1973.
(6) de la Mare, P. B. D.; Fowden, L.; Hughes, E. D.; Ingold, C. K.; Mackie, J. D. H. *J. Chem. Soc.* **1955**, 3200.
(7) (a) Parker, A. J. *Chem. Rev.* **1969**, *69*, 1. (b) Cook, D.; Parker, A. J. *J. Chem. Soc. B* **1968**, 142.
(8) DeTar, D. F.; McMullen, D. F.; Luthra, N. P. *J. Am. Chem. Soc.* **1978**, *100*, 2484.
(9) (a) Dedieu, A.; Veillard, A. *J. Am. Chem. Soc.* **1972**, *94*, 6730. (b) van der Lugt, W. Th. A. M.; Ros. P. *Chem. Phys. Lett.* **1969**, *4*, 389. (c) Mulder, J. J. C.; Wright J. S. *Ibid.* **1970**, *5*, 445. (d) Ritchie, D. D.; Chappell, G. A. *J. Am. Chem. Soc.* **1970**, *92*, 1819. (e) Dyczmons, V.; Kutzelnigg, W. *Theor. Chim. Acta* **1974**, *33*, 239. (f) Baybutt, P. *Mol. Phys.* **1975**, *29*, 389. (g) Keil, F.; Ahlrichs, R. *J. Am. Chem. Soc.* **1976**, *98*, 4787. (h) Bader, R. F. W.; Duke, A. J.; Messer, R. R. *Ibid.* **1973**, *95*, 7715. (i) Schlegel, H. B.; Mislow, K.; Bernardi, F.; Bottoni, A. *Theor. Chim. Acta* **1977**, *44*, 245. (j) Ishida, K.; Morokuma, K.; Komornicki, A. *J. Chem. Phys.* **1977**, *66*, 2153.
(10) Wolfe, S.; Mitchell, D. J.; Schlegel, J. H. *J. Am. Chem. Soc.* **1981**, *103*, 7692, 7694.
(11) (a) Farneth, W. E.; Brauman, J. I. *J. Am. Chem. Soc.* **1976**, *98*, 5546. (b) Olmstead, W. N.; Brauman, J. I. *J. Am. Chem. Soc.* **1977**, *99*, 4219. (c) *Ibid.* **1979**, *101*, 3715.
(12) Hiraoka, K.; Kebarle, P. *J. Am. Chem. Soc.* **1976**, *98*, 6119; *Can. J. Chem.* **1980**, *58*, 2262.
(13) Hiraoka, K.; Kebarle, P. *Radiat. Phys. Chem.* **1982**, *1*, 41.
(14) Sen Sharma, D. K.; Kebarle, P. *J. Am. Chem. Soc.* **1982**, *104*, 19.
(15) Magnera, T. F.; Kebarle, P. In Ionic Processes in the Gas Phase"; Almoster Fereira, M., Ed.; D. Reidel Publishing Co.: Dordrecht, The Netherlands, 1984; NATO ASI Series, Vol. 118, p 135. Vol. 118, p 135.

The first systematic studies of gas-phase S_N2 reactions were reported by Bohme and co-workers.[16] Many of the reactions were found to proceed with rate constants significantly lower than the orbiting collision rate constants. However, all the determinations were performed at room temperature. At the time when these studies were undertaken it was often assumed[16c,17] that reaction inefficiency was due to a positive ΔE_0. Solomon, Meot-Ner, and Field,[18] who studied the hydride transfer reaction 3, were the first

$$R_0^+ + RH = R_0H + R^+ \quad (3)$$

to show that reactions with low collision efficiencies also can have negative temperature dependence. Olmstead and Brauman[11] made an experimental and theoretical study of several gas-phase S_N2 reactions. The idea that the reaction can have a low collision efficiency even when ΔE_0 is negative because a bottleneck develops at the tight chemical transition complex was clearly stated in that work[11] for the first time.

Olmstead and Brauman compared the rate constants, which they had measured at a single temperature, with calculated rate constants. Passage over the chemical transition state was treated with RRKM formalism. They evaluated ΔE_0 for a few reactions by selecting values for ΔE_0 in the calculation that led to agreement with the experimentally measured rate constant. The values obtained for ΔE_0 were negative.

Evaluations of ΔE_0 by fitting the calculations to the experimental rate constants at a single temperature rely totally on the adequacy of the model calculation used. Much more convincing of the applicability of the calculations would be to obtain a fit of the theoretical rate constants calculated for different temperatures to the experimentally measured rate constants at the corresponding temperatures.

The first measurement of the temperature dependence of S_N2-type reactions was reported recently from this laboratory.[14] The reaction series involved was the nucleophilic attack of netural bases B on the dimethylchloronium ion represented in eq 4. The

$$B + MeClMe^+ = BMe^+ + ClMe \quad (4)$$

$$B = Me_3N,\ NH_3,\ O(Me)_2,\ O(Et)_2,\ i\text{-}PrC_6H_5,\ EtC_6H_5,\ C_6H_6$$

chemical transition state in reaction 4 should be very similar to that represented in I with B replacing Cl^- and ClMe replacing Br^-. The reaction series 4 gave a very convincing demonstration of the reality of the reaction coordinate model of Figure 1. The top of the chemical barrier can be expected to go up as the basicity of B decreases, i.e., in the order given in (4). In agreement with this expectation and the previous discussion, k_4 for the strongest nucleophiles Me_3N and H_3N was found to be approximately equal to k_L and temperature independent; the somewhat weaker Me_2O and Et_2O had $k_4 < k_L$ and negative temperature dependence with k_4 becoming equal to k_L at low temperatures. For the alkyl benzenes, k_4 was much less than k_L and had negative temperature dependence while the weakest nucleophile benzene had the lowest k_4 and *positive* temperature dependence. Evidently for benzene the top of the barrier had just penetrated above the energy level of the reactants, i.e., ΔE_0 had just become positive. RRKM calculations following the Brauman model[11] were not performed for reaction 4 since the necessary vibrational frequencies and geometric information on Me_2Cl^+ and the transition state were not available. However, the calculations of Brauman[11] for some of the S_N2 reactions involving negative ion reaction 2 were extended to temperatures other than room temperature.[15] As expected,[12,14] the negative ΔE_0 were found to lead to negative temperature dependence. Obviously, it is of great interest to check how well these calculations agree with an experimentally measured temperature dependence. This interest provided the second impetus for the present work.

Experimental and Calculations

(a) Experimental. The kinetic and equilibrium measurements were performed with a pulsed electron beam high ion source pressure mass spectrometer which was used in the earlier work[12-14] and has been described before. The experimental conditions for the present measurements were similar to those used in the earlier chloronium ion work.[14]

All the alkyl bomides were obtained commercially. The MeBr (Matheson) was used as is. The other alkyl bromides were purified by fractional distillation, and the purity of the fraction used was checked by GC-MS analysis. After distillation, only the *t*-BuBr sample contained an impurity of empirical formula C_4H_9OBr. It appeared that this impurity was involved in a Br^--producing reaction in the presence of Cl^-. Since S_N2 reaction 2 to be studied with *t*-BuBr was expected to be very slow and the impurity was difficult to remove completely, experiments with *t*-BuBr were discontinued.

Since some of the rate measurements were carried to relatively high temperatures (370 °C), checks were made to establish that decomposition of RBr to HBr and other products did not occur. A quadrupole mass spectrometer mounted in the vacuum chamber was used to analyze the composition of the gases escaping from the heated ion source. Comparison of the mass spectra observed at low and high temperature showed that no thermal decomposition was occurring.

(b) Calculations. Calculations of the rate constants k_2 for MeBr and *n*-BuBr at different temperatures were performed for the chemically activated low-pressure case following the procedures of Olmstead and Brauman.[11] The frequencies and moments of inertia provided by these authors were used.

The usual adiabatic rotation correction used in the present calculation and by Brauman is to decrease $-\Delta E_0$ by the quantity $kT(I_L/I_T - 1)$, where I_L/I_T is the moment of inertia ratio of the loose orbiting and tight chemical transition state. Brauman had selected $I_L/I_T = 3$ at 300 K. We used the same value at this temperature. However, for calculations at different temperatures a problem arises. Since $k_L = k_{ADO}$ has a weak negative temperature dependence,[19] if one sets $k_{ADO} = \bar{v}_{rel}\pi r_L^2$, where $\bar{v}_{rel}$ is the average relative velocity and r_L is the radius of the loose complex, one obtains an r_L that decreases with an increase in temperature. This means that $I_L = \mu r_L^2$, where μ is the reduced mass of the quasi-bimolecular AB^- loose complex, also decreases with temperature. We calculated the temperature decrease of I_L in the above manner but assumed that I_T is temperature independent. Thus, in the present calculations $I_T/I_L = 3$ at 300 K and less than 3 at higher temperatures. This choice has a significant effect on the calculated temperature dependence of the rate constants. Rate constants calculated with the assumption I_L/I_T = constant at all temperatures were also made.

Results and Discussion

(a) Measurements of Rate Constants for Reaction 2: Cl^- + RBr = ClR + Br^-. The rate constants were measured by observing the decay of Cl^- after the short electron pulse (10 μs) in which Cl^- was produced by dissociative attachment of near-thermalized electrons to CCl_4

$$e + CCl_4 = Cl^- + \cdot CCl_3 \quad (5)$$

The reaction mixtures, subjected to electron pulses, consisted of CH_4 as a major gas, at a known pressure in the 3–6-torr range, containing known pressures of RBr, in the mtorr range, and CCl_4, at 0.1 mtorr. Under these conditions, the only initial ion observed was Cl^-. Examples of the Cl^- decay with time are shown in Figure 2. The slowest decay (run A) was observed in the absence of reactant RBr and represents the decay due to diffusive loss of Cl^- to the walls of the ion source. The progressively more rapid decay in runs B to E was observed with known RBr concentrations which were increased from B to E. Since the diffusive ion loss is inversely proportional to the total ion pressure, a series of runs like those shown in Figure 2 was performed at constant total pressure. The diffusive loss is also expected to depend on the composition of the gas mixture; however, since in all measurements methane represented more than 90% of the total gas, one expects that the diffusive changes with [RBr] change will have a negligible effect on the reaction rate measurements.

The slopes of the linear portions of the log (I_{Cl^-}) versus t plots of Figure 2 which equal the (pseudo)-first-order rate constants for Cl^- disappearance [= ν (s^{-1})] are shown in Figure 3. The ν of run A ([RBr] = 0) is due to diffusive loss while the ν's for

(16) (a) Bohme, D. K.; Young, L. B. *J. Am. Chem. Soc.* **1970**, *92*, 7354. (b) Young, L. B.; Lee-Ruff, E.; Bohme, D. K. *J. Chem. Soc., Chem. Commun.* **1973**, 35. (c) Bohme, D. K.; Mackay, G. I.; Payzant, J. D. *J. Am. Chem. Soc.* **1974**, *96*, 4017. (d) Bohme, D. K.; Mackay, G. I.; Tanner, S. D. *Ibid.* **1980**, *102*, 407. (e) Tanaka, K.; Mackay, G. I.; Payzant, J. D.; Bohme, D. K. *Can. J. Chem.* **1976**, *54*, 1643.

(17) Ausloos, P.; Lias, S. G. *J. Am. Chem. Soc.* **1970**, *92*, 5037.

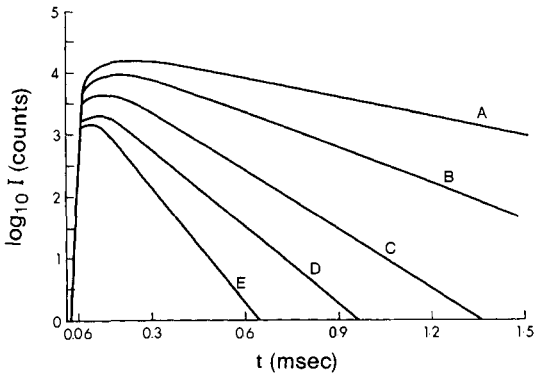

Figure 2. Ion intensity of Cl^- as a function of time after a 10-μs electron pulse observed at a constant ion source temperature of 329 K and a constant total pressure with reaction mixtures containing 5 torr of CH_4 and increasing concentrations of CH_3Br. $[CH_3Br] = 0$ for A and maximum for E. For actual concentrations, see Figure 3. The Cl^- ion is produced during the electron pulse from dissociative electron capture by CCl_4 ($p(CCl_4) \approx 0.1$ mtorr). The Cl^- ion decay in A represents loss due to diffusion of Cl^- to the ion source walls. The progressively more rapid decays in runs B to E are due to the reaction $Cl^- + CH_3Br = ClCH_3 + Br^-$ and the small, presumed constant, diffusive ion loss.

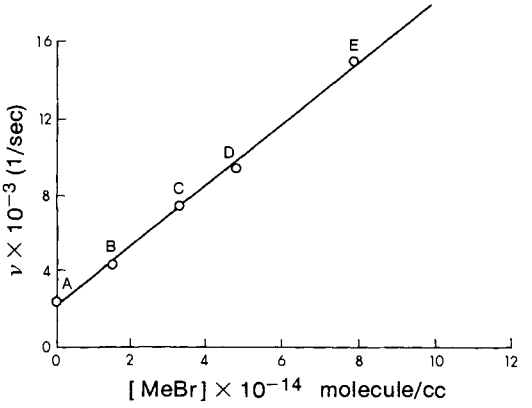

Figure 3. Plot of reaction frequencies ν (pseudo-first-order rate constants) obtained from slopes of the linear portions of runs shown in Figure 2. ν for run A represents pure diffusive loss while ν's for runs B to E include reactive loss of Cl^- due to the reaction $Cl^- + CH_3Br = ClCH_3 + Br^-$. The slope of the straight line leads to the rate constant $k = 1.7 \times 10^{-11}$ cm^3 molecule^{-1} s^{-1} at 329 K.

the other runs reflect a progressively increasing reactive loss on top of the assumed constant diffusive loss. The slope of the straight line in Figure 3 gives the rate constant k_2 for reaction 2.

A plot of the observed ions in percent of the ion total vs. time is shown in Figure 4. The observed ion intensity changes with time show that Br^- is the only significant product of the reactive disappearance of Cl^-. The few minor products observed at longer reaction times like $Cl^-(H_2O)$, $Br^-(H_2O)$, and Cl^-CCl_4 are clearly insignificant compared with the major product Br^-.

Measurements like those illustrated in Figures 2–4 were performed at different temperatures. An example of a plot analogous to Figure 3, but with measurements at different temperatures with RBr = *i*-PrBr, is shown in Figure 5. The rate constants, corresponding to the slopes obtained at different temperatures, are clearly seen to increase with an increase of temperature. Evidently, this reaction has positive temperature dependence.

Arrhenius plots for the rate constants k_2 obtained by the procedures illustrated in Figures 2–5 are shown in Figure 6. The plots are seen to be linear within the experimentally accessible range. The plots divide into two groups. The first group, consisting of the secondary bromides, *i*-PrBr and *i*-BuBr, has significant positive temperature dependence. Very weak temperature dependence is observed for the second group containing the primary bromides, MeBr, EtBr, and *n*-BuBr. The temperature dependence for MeBr is negative and that for EtBr weakly positive, while *n*-BuBr shows essentially no temperature dependence. The

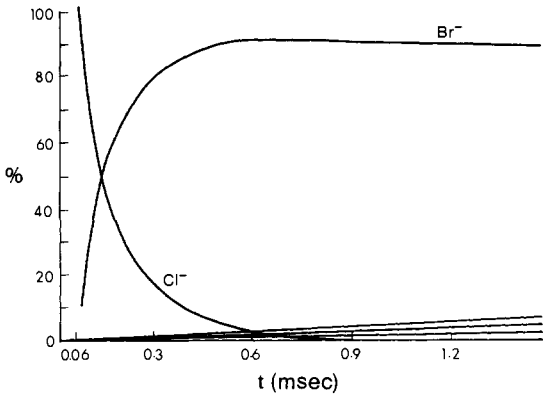

Figure 4. Plot of the observed ions in percent of total ion current as a function of time after the electron pulse for run D of Figures 2 and 3. Observed ion intensity changes show that Br^- is the only ion product of any significance coupled to the disappearance of Cl^-. The reaction involved must be $Cl^- + MeBr = ClMe + Br^-$. The minor products observed at long reaction times are $Cl^-\cdot H_2O$, $Br^-\cdot H_2O$, and $Cl^-\cdot CCl_4$ in order of decreasing concentrations.

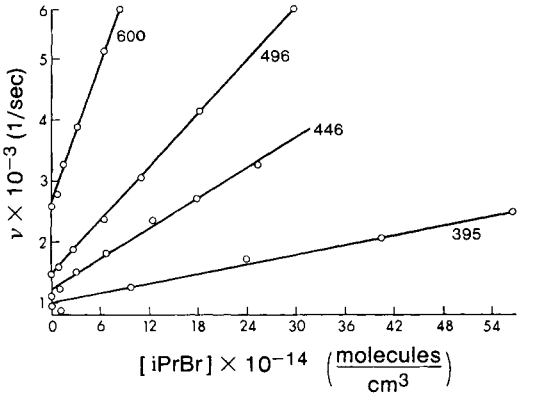

Figure 5. Plot of Cl^- ion loss frequencies ν measured in runs analogous to those shown in Figures 2–4 but with i-PrBr as the reactant gas. Slopes of the straight lines give rate constants for the reaction $Cl^- + i\text{-}PrBr = i\text{-}PrCl + Br^-$. The different temperatures (K) used are given in the figure. The increasing slopes with increasing temperature show that the rate constant for this reaction increases with temperature.

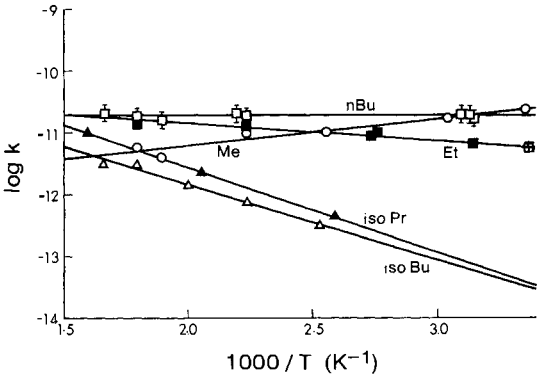

Figure 6. Arrhenius plots of S_N2 reaction rate constants k_2: $Cl^- + RBr = ClR + Br^-$. Reactions fall into two groups: R = Me (○), Et (■), and *n*-Bu (□), the primary alkyl groups, with small negative or positive temperature dependence; and R = i-Pr (△) and *i*-Bu (▲) with significant positive temperature dependence. The Arrhenius parameters obtained are shown in Table I. The reaction coordinate deduced for Me is shown in Figure 1. The adduct concentrations $[Cl^-RBr]$ were very small in all runs except for the lowest temperature determination for EtBr (⊞). This result was obtained from data in Figure 10.

preexponential factors and activation energies obtained from Figure 6 are given in Table I.

Rate-constant measurements also were attempted for *t*-BuBr. However, the rate of the S_N2 reaction proved difficult to measure. From the trends observed above, one expects k_2 (*t*-BuBr) to be

Table I. Values from Arrhenius Plots of Rate Constants $k_2 = A_2 e^{-E_2/RT}$ for Gas-Phase Reaction 2: $Cl^- + RBr = ClR + Br^-$

R	$-\log A_2$,[a] cm^3 molecule^{-1} s^{-1}	E_2[a]	$\sim\Delta E_0$[b]	$-\Delta H_2°$[c]	$-\Delta G_8°$[d]
Me	12.1	−1.9	−2.5	8.0	
Et	10.3	1.3	0.8	7.4	6.7
n-Pr				7.0	7.5
n-Bu	10.7	0.0	−0.5	6.0	7.6
s-Bu					7.5
i-Pr	9.9	5.6	5.1	6.6	7.8
i-Bu	8.8	6.2	5.7	6.2	8.1
t-bu				8.3	8.6

[a] From Arrhenius plots, Figure 6. [b] kcal/mol. Estimated ΔE_0 obtained by subtracting 0.5 kcal/mol from E_2. This is an approximate correction for temperature dependence of A_2 (see text). Slightly different values were obtained for Me and *n*-Bu from calculations, see Figures 7 and 8. ΔE_0 is defined in Figure 1. [c] kcal/mol. Enthalpy change for reaction 2. ΔH_f for RBr and RCl from Cox and Pilcher: Cox, J. D.; Pilcher, G "Thermochemistry of Organic and Organometallic Compounds"; Academic Press: New York, 1970. $\Delta H_f(Cl^-) = -55.9$, $\Delta H_f(Br^-) = 52.4$ kcal/mol. [d] Free energy change for adduct formation, eq 8: $Cl^- + RBr = Cl^-RBr$. From equilibrium constants, see Figure 9. Temperature 304 K; standard state 1 atm.

much smaller than the k_2 for the other compounds. This means that the *t*-BuBr must be of very high purity. Unfortunately, the GC-MS analysis of the *t*-BuBr showed that this compound contained an impurity C_4H_9OBr and this impurity was difficult to remove by distillation (see Experimental section). It appeared that Br^- was produced from this impurity. Therefore, the measurements with *t*-BuBr could not be performed. We hope to report on measurements involving this compound and other sterically hindered compounds like 1-bromoadamantane at a later date.

(b) Interpretation of the Temperature Dependence of the Rate Constants: Pressure Effects, Boltzmann Distribution, or Chemical Activation. The Arrhenius plots in Figure 6 for the *i*-PrBr and *i*-BuBr have positive temperature dependence. The Arrhenius activation energies obtained from the plots are 5.6 and 6.2 kcal/mol, respectively. We conclude that for these compounds ΔE_0 is positive, i.e., the energy of transition-state I is higher than the energy of the reactants (Figure 1). For these compounds, passage over the central barrier is possible only when thermal activation is present. Therefore, the conventional TST equation (eq 6) should apply.[19] Since the Arrhenius activation energy for

$$k_{TST} = \frac{kT}{h}\frac{Q_{AB^*}}{Q_A Q_B}\exp(-\Delta E_0/RT) \qquad (6)$$

both reactions is rather small, the temperature dependence of the preexponential factor needs to be considered. Qualitatively it is easy to show that the temperature dependence predicted by (6) is small, i.e., approximately $\propto T^{1/2}$. On formation of transition state I, three totally new vibrations are created. Assuming that one of these is the reaction coordinate the remaining two can be identified with two weak bending vibrations (approximately 300 cm^{-1}) of the two halogen atoms with the alkyl group representing the central "atom". The partition functions of these two vibrations have a temperature dependence of about $T^{1/2}$ each in the temperature range used. Since the temperature dependence of the partition functions of the external rotations cancel and the translational contribution is $T^{-3/2}$, substitution into eq 6 leads to an approximate overall dependence of $T^{1/2}$. This dependence expressed as an exponential dependence, $\exp(-\alpha/RT)$, leads to an $\alpha \approx 0.5$ kcal/mol. We conclude that the Arrhenius activation energies for the secondary bromides are close to the ΔE_0 values and that subtracting 0.5 kcal/mol from the Arrhenius activation energies should lead to an approximate ΔE_0. Of the primary bromides, EtBr was found to have weak positive temperature dependence. For this compound, ΔE_0 should be close to zero and eq 6 still applicable.

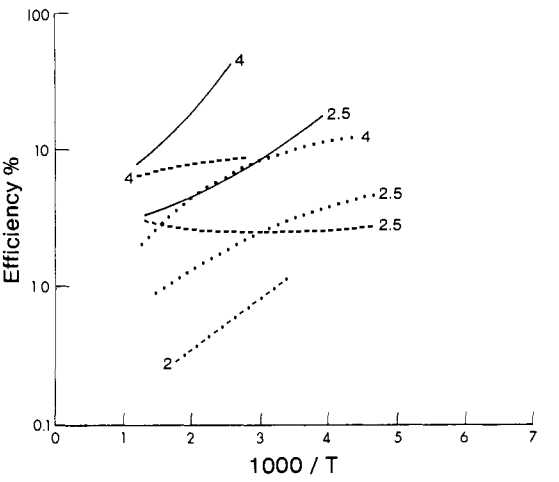

Figure 7. Comparison between experiment and theory for reaction 2, MeBr. eff: k_2/k_{ADO}. TST predictions (—) calculated with eq 6 should be a valid model at (infinitely) high pressure. The RRKM calculation for the low-pressure limit: RRKM(c) (···); RRKM(v) (- - -). The same frequencies were used as Brauman[11] used for TST and RRKM. The TST calculation with changed frequencies to obtain the complete fit of expeirmental results (-··-). The numbers given on the figure give values for $-\Delta E_0$ in kcal/mol.

We turn now to *n*-BuBr and MeBr which probably have small negative ΔE_0. At low pressures ($p \sim 10^{-6}$ torr) as used in ICR experiments,[11] reactions with negative ΔE_0 will proceed with chemical activation because no third-body collisions occur during the passage of the reactant pair through the reaction coordinate. That is, there is energy and angular momentum conservation for each microcanonical passage over the loose and tight transition state. In particular, the adduct A^-B (Cl^-RBr in the present case), which may be fairly long lived and either form the products (k_p) or back decompose (k_b) to the reactants (Figure 1), is not deactivated by collisions. As mentioned in the introduction, this low-pressure case was treated by Olmstead and Brauman,[11] who, using RRKM theory, evaluated k_p and k_b. They present their results in terms of the collision efficiency of the reaction which is defined by (7). Two of the three reactions treated by Brauman[11] were reaction 2 with R = Me and *n*-Bu. However, Brauman[11] reported calculated results only at room temperature.

$$A^- + B \underset{k_b}{\overset{k_c}{\rightleftharpoons}} (A^-B)^* \xrightarrow{k_p} \text{products} \qquad (7)$$

$$\text{eff} = \frac{k}{k_c} = \frac{k_p}{k_b + k_p} \qquad k_c = k_L$$

We have extended these calculations over a range of temperatures using the vibrational frequencies and equations provided by Brauman.[11] The results for MeBr and *n*-BuBr are shown in Figures 7 and 8. Results from two different RRKM calculations are shown. In RRKM(c) the ratio I_L/I_T used to correct for angular momentum conservation[11] was kept constant with temperature, while in RRKM(v) the ratio was changed with temperature (see section calculations). As is evident from Figures 7 and 8, quite different results are obtained. While neither correction is truly satisfactory, the simpler assumption used in RRKM(c) probably should be preferred. We shall base the further discussion on the RRKM(c) results alone. Also shown in these figures are rate constants evaluated with the macrocanonical TST, eq 6, using the same basic data, i.e., frequencies and

(18) Solomon, J. J.; Meot-Ner, M.; Field, F. H. *J. Am. Chem. Soc.* **1974**, *96*, 3727.

(19) (a) Bowers, M. T. In "Gas Phase Ion Chemistry"; Bowers, M. T., Ed.; Academic Press: New York, 1979. (b) The present reactions probably proceed via a relatively long lived complex $(AB)^*$ as shown in reaction scheme 7. According to this scheme $k \approx k_p$ when $k_p \gg k_b$. For this condition and thermally activated reactants, k can be evaluated by (6). The condition $k_p \gg k_b$ is present for most of the reactions under discussion, since the experimentally measured rate constant k is found to be orders of magnitude smaller than $k_c \approx k_L$.

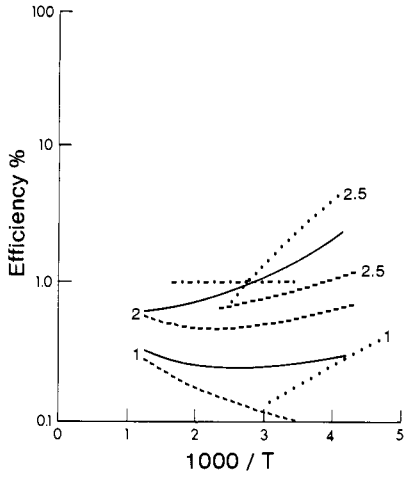

Figure 8. Comparison between experiment and theory for reaction 2, *n*-BuBr. eff = k_2/k_{ADO}. TST predictions (—); RRKM predictions RRKM(c) (···) and RRKM(v) (---); experimental results (-·-). The numbers given on the figure are values for $-\Delta E_0$ in kcal/mol.

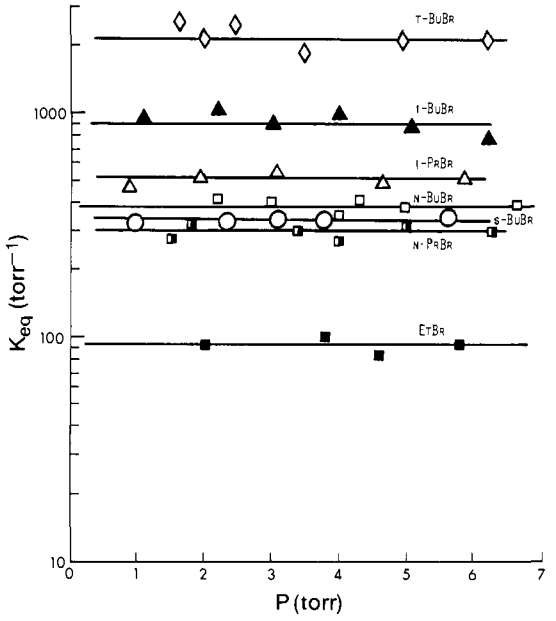

Figure 9. Equilibrium constants for adduct-forming reactions, Cl^- + RBr = Cl^-RBr, versus ion source pressure at temperature 304 K: (◇) *t*-BuBr, (▲) *i*-BuBr, (△) *i*-PrBr, (□) *n*-BuBr, (○) *s*-BuBr, (◨) *n*-PrBr, (■) EtBr. Equilibrium was not observed for MeBr.

moments of inertia for transition-state **I** and reactants. Additional details about the calculations are given in the Experimental and Calculations section. ΔE_0 has been used as a variable parameter in both sets of calculations.

The present experimental results were obtained at much higher pressures (~4 torr) than the ICR results (10^{-5}–10^{-6} torr). The question arises, which model—low-pressure RRKM with chemical activation or high-pressure, thermal TST (eq 6)—should be applied?

A strong indication that the experiments are closer to the TST model is given by the observation that the adducts Cl^-RBr were thermalized at least at the low-temperature end of the experiments. The adducts Cl^-RBr were not only observed but also the equilibrium constants for their formation by (8) could be measured for all cases but MeBr. The equilibrium constants K_8 were found

$$Cl^- + RBr = Cl^-RBr \qquad (8)$$

to be independent of the third gas pressure (Figure 9), a good proof that the thermalization of the adduct Cl^-RBr was complete. An equilibrium constant could not be determined for MeBr. For this compound, the observed concentration ratio of Cl^- and adduct

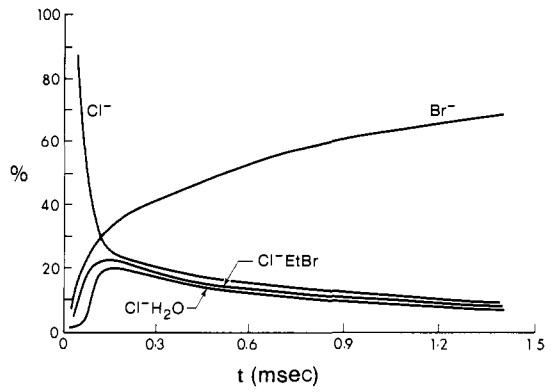

Figure 10. Ion intensities for the experiment with EtBr at 303 K. The initial rapid fall off of Cl^- corresponds to a buildup of adduct Cl^-EtBr up to the equilibrium concentration. After ~0.2 ms the adduct equilibrium is established. Cl^- and Cl^-EtBr continue to decrease because of continued formation of Br^- via reaction 2: Cl^- + EtBr = ClEt + Br^-. A small amount of Cl^-H_2O is also formed due to the presence of a small water impurity. The shape of the concentrations of Cl^-EtBr and Cl^-H_2O at short reaction times clearly shows that the hydrate is formed after Cl^-EtBr, i.e., by the switching reaction $Cl^-EtBr + H_2O = Cl^-H_2O$ + EtBr.

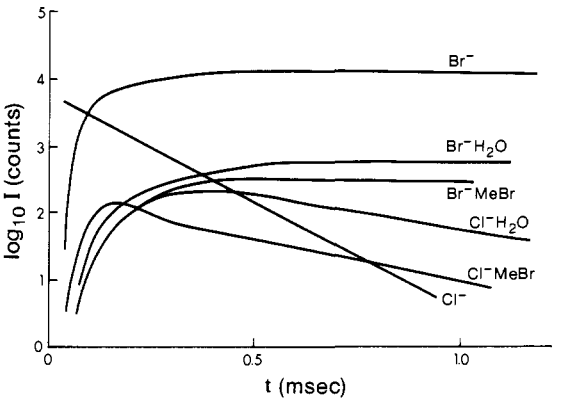

Figure 11. Ion intensities observed for reaction 2, MeBr, at 303 K. The different slopes of Cl^- and Cl^-MeBr show that the concentration ratio for these two ions does not become constant at longer reaction times. This means that an adduct equilibrium Cl^- + MeBr = Cl^-MeBr is not established at this temperature.

Cl^-MeBr did not become constant at long reaction time. A comparison of the time-dependent ion intensities in EtBr where equilibrium 8 was achieved and MeBr where equilibrium was not achieved is shown in Figures 10 and 11. We assume that if equilibrium 8 can be observed thermal TST eq 6 will be applicable even when ΔE_0 is negative. Thus, eq 6 should be applicable for the *n*-BuBr results.

Even though equilibrium 8 was not observed for MeBr, the fact that the concentration of the adduct Cl^-MeBr was high enough to be detected (Figure 11) means that a significant fraction of the chemically activated $(Cl^-MeBr)^*$ was at least partially thermalized. While TST eq 6 cannot be assumed to apply to these experiments, this model is probably closer to the experimental conditions than the chemically activated RRKM scheme (eq 7). On principle, the presence of collisional stabilization could be treated theoretically by including reaction 9 into mechanism 7.

$$(A^-B)^* + M \underset{k_a}{\overset{k_s}{\rightleftharpoons}} A^-B + M \qquad (9)$$

The present experimental results do not extend to sufficiently low pressures to provide an experimental check on theoretical results for mechanisms 7 + 9. In the absence of experimental data, it does not seem worthwhile to pursue the much more complex treatment of (7) + (9).

The theoretical results, RRKM and TST, for MeBr (Figure 7) predict negative temperature dependence only when $-\Delta E_0$ gets bigger than approximately 2 kcal/mol. The TST slope closest

to the experimental slope is observed for $\Delta E_0 = -2.5$ kcal/mol. The absolute values of these theoretical efficiencies are about a factor of 10 higher than the experimental values. It is possible to obtain better agreement between the TST predictions and the experimental results by tightening some of the frequencies used in the calculation. By replacing the three softest frequencies (300 cm^{-1}) with 600 cm^{-1} and choosing $\Delta E_0 \approx -2$ kcal/mol, one obtains complete agreement with experiment (see Figure 7).

Experimental determinations of k_2(MeBr) at 300 K have been reported by Olmstead and Brauman[11] and Tanaka, Bohme, et al.[16] The values for $k_2 \times 10^{11}$ (molecule^{-1} cm^3 s^{-1}) are as follows: 2.4 (present work), 2.1 (Bohme), and 1.2 (Brauman). The differences are essentially within the experimental error of the measurements. However, exactly such differences can be expected as a result of the different pressures used in the different measurements. For reactions with negative ΔE_0, one can expect that any collisional cooling of the excited A^-B adduct will decrease k_b more than k_p (see Figure 1) and thus result in an increase of the overall rate constant. The higher k_2(MeBr) determined in the higher pressure experiments of Bohme (Flowing afterglow $p \approx 0.5$ torr) and the present work ($\sim$5 torr) as compared to the ICR measurements[11] ($p \approx 10^{-5}$ torr) may be due to exactly such an effect. The theoretical results TST and RRKM(c) for a $\Delta E_0 = -2$ to -2.5 kcal/mol at 300 K (Figure 7) predict a ratio for the high-pressure to low-pressure k_2 of about 2. This is in agreement with the experimental results discussed above. The close agreement is probably fortuitous since the model calculations are quite crude.

The low-pressure RRKM and the high-pressure TST results determine the low- and high-pressure limits of the rate constant. At intermediate pressures the rate constant will be pressure dependent. However, for the present case (MeBr), assuming that the calculations are at least qualitatively correct, that pressure dependence will be difficult to detect since the difference between the high pressure and low pressure limit rate constants is so small. There should be reactions for which that difference is much larger. Therefore, one should bear in mind that rate constants for bimolecular rate constants of inefficient reactions with negative ΔE_0 may differ depending on the pressure required by the experimental method used, i.e., ICR (low-pressure limit), flowing afterglow, and high pressure MS, nearer to the high-pressure limit. The comparisons between theory and experiment in Figure 7 demonstrate the desirability for experimental results at low and high pressure and at different temperatures for this and other reactions. Only such data will permit a more rigorous test of the theoretical models used.

The RRKM, TST, and experimental results for *n*-BuBr are shown in Figure 8 where the theoretical results use the frequencies provided by Brauman.[11] As discussed above, TST probably applies for the present experimental conditions. The TST slope closest to the experimental result is for $\Delta E_0 \approx -1$ kcal/mol. The absolute values of the theoretical efficiences for this ΔE_0 are about a factor of 4 lower than the experimental results. Thus, loosening of some of the frequencies used and decreasing $-\Delta E_0$ somewhat should lead to approximate agreement with experiment.

We have not extended the calculations to include all RBr for which measurements were made. The compounds with negative ΔE_0 for which calculations were made are the more interesting cases. Since the frequencies for the transition states have to be estimated, special insights for the remaining systems probably will not be provided by the calculations.

The kinetics of the reactions where substantial amounts of the adduct Cl^-RBr are formed and equilibrium 8 between Cl^- and adduct is established, for an example see Figure 10, are interesting and deserve some comment. Early in the reaction, the concentration of the adduct is being built up and the decrease of Cl^- does not reflect the rate of S_N2 reaction 2. However, after equilibrium 8 is established, the rate of Cl^- disappearance should correspond to the rate of (2). A k_2(EtBr) could be evaluated from Figure 10 by using the integral plot technique[20] over the range where Cl^- was in equilibrium with Cl^-EtBr. This value shown as the lowest temperature point in the Arrhenius plot of the reaction (Figure 6) is seen to fit well on the line, a result that further confirms the thermal nature of reaction 2 for these conditions. One may also take the viewpoint that the reaction does not occur from Cl^- but from the observed complex Cl^-RBr. Of course, the dissociation to Br^- + RCl out of the complex will be strongly endothermic (Figure 1). However, since the concentration of the complex is related to the concentration of the reactants Cl^- and RBr via equilibrium 8, the strongly negative temperature dependence of that equilibrium when combined with the positive temperature dependence of the dissociation from the complex leads to the observed small temperature dependence of k_2.

The experimental results and the rate measurements, Figures 1–6 and Table I, are consistent only with a reaction in which Cl^- disappears and is replaced by Br^-. We have assumed that this change is due to S_N2 reaction 2. Unfortunately, the mass spectrometric detection used in the present work (as well as in ICR[11] and flowing afterglow[16] experiments) does not provide for detection and identification of the neutral products. Therefore one cannot be certain that the reactions involved are reaction 2. The only other reaction which has the same ionic reactants and may be considered likely in the gas phase is the second-order elimination process (E2) which is possible for alkyl bromides other than methyl bromide. For example, EtBr can lead to reaction 10. Alkyl

$$Cl^- + C_2H_5Br = HCl + C_2H_4 + Br^- \qquad (10)$$

bromides in solution react predominantly via the S_N2 route except the tertiary compounds like *t*-BuBr for which E2 dominates.[7,8] The enthalpy change for the E2 reactions in the gas phase can be evaluated by using enthalpies of formation from the literature (see footnote *c*, Table I). These ΔH values in kcal/mol are as follows: EtBr, 9.1; *n*-PrBr, 6.8; *n*-BuBr, 6.8; *i*-PrBr, 9.8; *i*-BuBr, 8.4. Since all these reactions are endothermic, they should proceed with positive temperature dependence, and the rate constants can be described by TST eq 6. The minimum activation energy expected is given by the ΔH for these reactions. Comparison with the activation energies from the Arrhenius plots, Table I, shows that the only reactions that have activation energies anywhere near the ΔH values are *i*-PrBr (E_a = 5.6 kcal/mol) and *i*-BuBr (E_a = 6.2 kcal/mol). We believe that the measured E_a for *i*-PrBr is still significantly lower than the ΔH of 9.8 kcal/mol and that the difference between the two values is outside our error of measurement. Therefore, the only compound for which the E2 reaction could be occurring is *i*-BuBr. None of the arguments and interpretations in the present work depend critically on whether this compound reacts via the S_N2 or E2 path.

It could be argued that the E2 elimination leads not to HCl and Br^- but to the strongly hydrogen bonded $(ClHBr)^-$ as shown in (11). This process is made exothermic by the hydrogen bond

$$Cl^- + C_2H_5Br = C_2H_4 + (ClHBr)^- \qquad (11)$$

energy of Br^-HCl which can be expected to be around 15 kcal/mol.[21] In fact, E2 reactions in which a strongly hydrogen bonded product is formed have been observed by Beauchamp,[22] Jennings,[23] and others. However, the observed reactions involve strong nucleophiles like F^- and RO^-. We should have been able to detect the presence of $ClHBr^-$ had reaction 11 occurred. A search was made but this ion was not detected.

(c) Comparison of Transition-State Energies in the Gas Phase and in Solution. The energy of transition state I relative to the reactants Cl^- and RBr obtained for the gas-phase reactions (see preceding section) is given in Table II. The zero-point energy of the transition state lies 2.5 kcal/mol below that of the reactants for MeBr and climbs to slightly below the reactants for *n*-BuBr and slightly above for EtBr and then some 5–6 kcal/mol above the reactants for *i*-Pr and *i*-Bu. Also given in Table II are the activation energies measured in *N,N*-dimethylformamide (DMF) solution by Parker and co-workers.[7] The energies of the transition states in solution are some 17 to 21 kcal/mol above those of the reactants. The much higher activation energy in solution must be primarily due to the lower solvation energy of the transition state ion $ClRBr^-$ relative to that for the much smaller Cl^- ion. The differences of activation energies for different RBr are also shown in Table II. The $\delta\Delta H^*$ in solution shown in the table are

Table II. Energies of Transition States for S_N2 Reactions: Gas Phase, Solution, and Calculation

	ΔE_0[a] gas phase	$\Delta H^{\ddagger}$[b] DMF	ΔE_{st}[c] DeTar	$\delta\Delta E_0$[d] gas phase	$\delta\Delta H^{\ddagger}$[e] soln	$\delta\Delta E^f_{st}$ DeTar	$\delta\Delta E^f_{st}$ Ingold
Me	−2.5	17.7	7.4	0	0	0	0
Et	0.8	18.5	13.6	+3.3	+2.4	+6.2	+1.9
n-Pr		17.4	13.7		2.7	+6.3	1.9
n-Bu	−0.5			+2.0			
i-Pr	+5.1	20.6	17.8	7.6	5.0	10.4	3.3
i-Bu	+5.7	18.8	15.5	8.2	4.4	8.1	3.2

[a] Present results for the gas-phase reaction $Cl^- + RBr = ClR + Br^-$. ΔE_0 denotes the zero-point difference between reactants and the transition state on top of the central barrier in Fibure 1. Estimated error ±0.5 kcal/mol. [b] Results of Parker[7] for the reaction $Cl^- + RBr = ClR + Br^-$ in *N*,*N*-dimethylformamide (DMF). [c] Calculated steric energy due to repulsions in transition-state Br--R--Br, relative to reactants, from Table IV of DeTar.[8] [d] Differences $\Delta E_0(RBr) - \Delta E_0(MeBr)$ from the gas-phase data column II. [e] Differences of activation energies for the reaction $Cl^- + RBr = ClR + Br^-$ in solution. Analysis of experimental data by DeTar, Table II in ref 8. [f] Steric strain energy calculations relative to ΔE_0(MeBr), DeTar[8] and Ingold.[6]

from an analysis of the solution data by DeTar.[8] Also given in Table II are results from the calculation of the steric strain present in the transition state relative to that in the reactant RBr. The calculation of Ingold[6] as well as the more recent, force field, molecular mechanics calculations of DeTar[8] are given. While there is considerable scatter in the four sets of $\delta\Delta$ values, on the whole the results are comparable and reflect the same trends. Thus, all four sets of data predict a jump of a few kcal/mol from Me to Et, a small change for β substitution, i.e., Et, *n*-Pr, *n*-Bu, and then another increase of a few kcal/mol for the second α substitution leading to isopropyl and isobutyl. This suggests that the activation energy differences in the gas phase and solution are due to the same cause, i.e., increasing steric repulsion between the two halide atoms and the alkyl groups in transition-state I. It should be noted that the steric strain calculations refer to $BrRBr^-$ and not to $ClRBr^-$. The steric energies for the dibromo complex should be somewhat larger; this should be taken into account when comparing the more recent and probably more reliable DeTar results for $\delta\Delta E_{st}$ with the experimental $\delta\Delta E_0$ and $\delta\Delta H^{\ddagger}$.

The steric strain calculations do not take at all into account the attractive interactions between the incoming halide ion and RBr. The attractive interactions lead to the formation of the adduct Cl^-RBr. The enthalpy change for the adduct formation $\Delta H_8°$ corresponds to the depth of the first well in Figure 1. In the preceding section Table I $\Delta G_8°$ measurements were reported. In some cases, these measurements could have been extended to obtain $\Delta H_8°$ values; however, fairly comprehensive determinations of binding enthalpy of Cl^- to different compounds are available in the literature.[21-23] On the basis of these determinations one can estimate that the average $-\Delta H_8°$ for the present reactions should be around 12 kcal/mol. A rough estimate of ΔE_0 in the gas phase may be obtained if one adds the calculated steric repulsion energies ΔE_{st}(DeTar) to $\Delta H_8°$. For example, for MeBr one obtains $\Delta E_0 \approx -12 + 7.5 = -4.5$ kcal/mol. The experimental $\delta\Delta G_8°$ in Table I may be taken as a measure of the $\delta\Delta H_8°$ values, since $\delta(T\Delta S_8°)$ is probably small. The experimental observation that ΔE_0(Et) − ΔE_0(*n*-Bu) ≈ 1.3 kcal/mol may be due to the fact that the well depth ΔH_8(*n*-Bu) is deeper than that for Et, i.e., $\Delta H_8°$(Et) − $\Delta H_8°$(*n*-Bu) ≈ 0.9 kcal/mol. Since the strain energies for these two compounds are expected to be the same (see ΔE_{strain} for Et and *n*-Pr, Table II), the $\delta\Delta H_8°$ should reflect the $\delta\Delta E_0$, and this is found, approximately, to be the case.

While there is a correspondence between the gas-phase $\delta\Delta E_0$ and the solution $\delta\Delta H^{\ddagger}$, an examination of the preexponential factors in the Arrhenius expression, $k_1 = A\exp(-E/RT)$, which are related to activation entropies, reveals a very different behavior between the gas phase and solution. In the gas phase, the preexponential factors are found to increase in the order Me, Et, *i*-Pr (see Table I) while in solution they decrease in the same order. For this reason the rate constants in the gas phase are found to obey the order observed in solution at room and lower temperatures but not at higher temperatures, where the entropy terms become dominant (see Figure 6). It is not clear to us whether the different activation entropies in the gas phase and solution are due to some unaccounted changes in solvation in the series Me, Et, *i*-Pr, ... or to some fundamental differences in the transition states for this series in the gas phase and in solution.

We believe that it is not worthwhile to speculate on what the exact causes may be; more desirable is further work on the temperature dependence of related gas-phase reactions and theoretical work: quantum chemical calculations of the transition states, e.g., F^-CH_3F vs. F^--*t*-C_4H_9F and kinetic theoretical development.

Conclusions

(a) The theoretical evaluation of the rate constant of a reaction like MeBr + Cl^- at a single temperature does not represent a sufficient test of the theoretical model; comparisons should be made at several temperatures.

(b) Reactions $A^{\pm} + B \rightarrow$ products with low collision efficiencies and small $-\Delta E_0$ can have pressure-dependent rate constants, since collisional quenching of the adduct $(AB^{\pm})^+$ favors product formation. ICR measurements should lead to the low-pressure limit (provided that the reactant ion is thermal) while flowing afterglow and high-pressure MS may be nearer to the high-pressure limit. The presence of deactivation is demonstrated by observation of the collision-stabilized adduct $AB^{\pm}$.

(c) The Cl^- + alkyl bromide reactions in the gas phase have internal energy barriers that increase by similar increments as the activation energies in solution and the classically calculated repulsion energies in the S_N2 transition state. However, the preexponential factors of the gas phase and solution rate constants change in opposite directions. The reasons for this latter difference of behavior are not clear.

Registry No. MeBr, 74-83-9; EtBr, 74-96-4; *n*-PrBr, 106-94-5; *n*-BuBr, 109-65-9; *sec*-BuBr, 78-76-2; *i*-PrBr, 75-26-3; *i*-BuBr, 78-77-3; *t*-BuBr, 507-19-7; Cl^-, 16887-00-6; CCl_4, 56-23-5.

(20) Lau, Y. K.; Ikuta, S.; Kebarle, P. *J. Am. Chem. Soc.* **1982**, *104*, 1462.
(21) Yamadagni, R.; Kebarle, P. *Can. J. Chem.* **1977**, *52*, 2449.
(22) Ridge, D. P.; Beauchamp, J. L. *J. Am. Chem. Soc.* **1974**, *96*, 379.
(23) Doorn, R. v.; Jennings, K. R. *Org. Mass. Spectrom.* **1981**, *169*, 397.
(24) French, M. A.; Ikuta, S.; Kebarle, P. *Can. J. Chem.* **1982**, *60*, 1907.
(25) Dougherty, R. C.; Dalton, J.; Roberts, J. D. *Org. Mass. Spectrom.* **1974**, *8*, 77.
(26) The bond dissociation enthalpy $D(Cl^-\cdots CH_3Cl)$ = 12 kcal/mol was determined recently by T. B. McMahon and J. W. Larson, private communication.